**Proceedings of ASME Turbo Expo 2011**
**GT2011**
**June 6-10, 2011, Vancouver, British Columbia, Canada**

**GT2011-45812**

# DETAILED LOCAL HEAT TRANSFER MEASUREMENTS IN A MODEL OF A DENDRITIC GAS TURBINE BLADE COOLING DESIGN

**James Batstone**
Department of Engineering Science,
University of Oxford, Oxford, UK

**David Gillespie**
Department of Engineering Science,
University of Oxford, Oxford, UK

**Eduardo Romero**
Rolls-Royce PLC
Bristol, UK

## ABSTRACT

A novel form of gas turbine blade or vane cooling in which passages repeatedly branch within the wall of the cooled component is introduced in this paper. These so called dendritic cooling geometries offer particular performance improvements compared to traditional cooling holes where the external cross flow is low, and conventional films have a tendency to lift off the surface. In these regions improved internal cooling efficiency is achieved, while the coolant film is ejected at a low momentum ratio resulting in reduced aerodynamic losses between the film and hot gases, and a more effective surface film. By varying the number of branches of the systems at a particular location it is possible to tune the flow and heat transfer to the requirements at that location whilst maintaining the pressure margin. The additional loss introduced using the internal branching structure allows a full film-coverage arrangement of holes at the external blade surface. In this paper the results of transient heat transfer experiments characterising the internal heat transfer coefficient distribution in large scale models of dendritic passages are reported. Experiments were conducted with 1, 2 and 3 internal flow branches at a range of engine representative Reynolds numbers and exit momentum ratios. CFD models are used to help explain the flow field in the cooling passages. Furthermore the sensitivity of the pressure loss to the blowing ratio at the exit of the cooling holes is characterised and found to be inversely proportional to the number of branches in the dendritic system. Surprisingly the highly branched systems generally do not exhibit the highest pressure losses.

## INTRODUCTION

A reduced and uncertain supply of oil combined with the environmental impact of burning fossil fuels necessitates the continuous improvement in modern aircraft engine propulsive efficiency. To this end there is a continuous need to increase specific thrust and reduce specific fuel consumption (SFC). There is a necessary pay off between increasing the engine pressure ratio and turbine entry temperature (TET) and the consequent increase in cooling mass flow rates required to maintain hot components within the metallurgical limits of the alloys available to manufacturers. Better cooling can be provided by maximising the cooling potential of air drawn from the compressor, and minimising the aerothermal penalty of its reintroduction into the mainstream. Of particular interest in this paper are the film cooling systems at the leading edge of high pressure nozzle guide vanes which currently rely on drilled holes fed from inside the vane. These are an area of particular concern as they sit in a highly turbulated flow field, with a low pressure margin driving the cooling flow and ejecting the film into a slow moving flow.

There have been numerous papers investigating the potential of novel film cooling designs e.g. Horlock, [1] , who considered the theoretical benefits of transpiration cooling. This is a process whereby the vane acts as if it were porous allowing the coolant to seep through the wall thus maximising heat pick up before it exits onto the vane surface at very low velocities normal to the surface. Near the leading edge this minimises mixing losses allowing a protective insulating film to form [2]. Although such a cooling strategy would produce optimum cooling it is not practical for an aircraft engine which is subject to particulate ingestion. Effusion cooling [3] is a cooling method where micro-holes are used which try to mimic some of the characteristics of transpiration cooling [4]. The diameter and spacing of the holes can be varied to suit the variation in pressure difference across the blade [3]. Again because of the small holes designs are susceptible to blockage.

Gillespie [5], Immarigeonk et al. [6] have presented film cooling strategies which involve impingement of air through an array of holes integral to the blade wall. Here, the wall is locally and substantially thickened, followed by ejection through a line of flared exit slots on the mid-span of the blade downstream of a structural pedestal bank. The large internal features increase internal heat transfer and allow the exit passage to be shaped to create an exit flow closely matched to the mainstream velocity. Sargison et al. [7] achieve similar flow velocity matching using a line of film-cooling holes whose shape is modified such that the exits form a slot. In this case velocity matching is achieved by reducing the passage width in the orthogonal direction such that the overall cross-sectional area reduces to minimise separation of flow in the hole; and to accelerate the flow back into the mainstream. One particularly attractive aspect of this design is its ability to achieve slot-like flow from discrete holes that will remain attached even at high momentum-flux ratios [8]. Further studies into console geometry were conducted by Liu et al. [9] who investigated the effect of momentum ratio and the console's divergence angle on the film performance. This study found that although far downstream film behaviour was broadly unaffected by the divergence angle, near the slot exit the angle determined the position of peak effectiveness. This study also concluded that at higher momentum ratios film lift-off still occurs and that the optimum momentum ratio with the highest average effectiveness for a console with an inclination of 35 degrees was 2.

This study preceded a comparative one, again by Liu et al. [10], that presented film cooling results of both straight holes and consoles arranged around a vane. There were 10 sets of cooling holes with the consoles at a 45deg. inclination. This study found that the consoles performed better at all momentum ratios. On the pressure surface the film performance was found to improve notably with coolant flow, conversely on the suction surface the performance was found to peak, after which it tails off at higher coolant flow rates. The reduction in film effectiveness was attributed to the separation of the film because of the convex nature of the suction surface.

While such schemes work on the midspan of the vane, at the leading edge ejection of coolant is more problematic, as the momentum ratio of flow exiting is likely to be much greater than unity. The so called Leading Edge Lattice (LEL), which consists of interesting film cooling passages arranged around the leading edge, is an example of such a scheme [11]. The LEL scheme, which utilises high internal loss, demonstrates little variation in flow and this results in less cyclical heating and thus potentially a longer component lifespan. Of particular note is the reduction to the stagnation region bulk blade metal temperature and the reduced coolant levels required by using such a scheme compared to conventional films.

Dierberger et al. [12] developed a cooling strategy which combines both impingement and transpiration cooling whilst being locally tuneable to the pressure difference available across the vane wall. The system consists of chambers within the wall; the inner wall has holes in through which the coolant jets and impinges on the outer wall which has holes in through which the coolant transpires. The tuning element of the system comes from the ability to vary the ratio of the total area of the impingement holes to the total area of the transpiration holes for each separate chamber.

To achieve an improvement over traditional film cooling holes in the leading edge region a cooling system should aim to have high internal convective efficiency, external film-cooling effectiveness and sufficient pressure margin to avoid ingestion. Additionally it must have low aero-dynamic loss for the flow in the mainstream gas path. High convective cooling efficiency is frequently achieved by maximising the cooling hole length to diameter ratio and slowing the flow within the holes. Maximum external cooling occurs where a thick layer of coolant is ejected which remains attached to the component surface: this requires the exit velocity of each cooling row to be scaled to the local cross-flow conditions, and to be injected at a streamwise oblique angle. Internal cooling features should be situated close to the outer surface to maximise their benefit (e.g. impingement).

A dendritic cooling system is one in which a cooling hole branches, possibly multiple times, and at each branch the passage bifurcates. The area of each exiting branch is equal to that of the incoming hole. The branching allows: the exit velocity to be tuned by changing the number of branches; maximisation of internal heat pick up through extension of the passage length for a given vane wall thickness; and improved pressure margin through the introduction of finite loss. A key feature is that the passage cross sectional area remains constant throughout: this avoids some of the blockage problems associated with previous cooling designs reporting to provide near transpiration cooling. The repeated halving of the flow velocity is particularly advantageous if used in the leading edge region where the mainstream is slow moving and film-attachment is conventionally difficult to achieve. The single inlet hole feeding the dendrite allows the flow to be metered accurately.

Figure 1 shows a typical design of a dendritic cooling system with repeatedly branching circular hole configurations with up to 8 outlets from a single inlet: note the naming convention which is used subsequently. The number of branches that can be accommodated is largely a function of the wall thickness of the engine component which requires cooling.

 

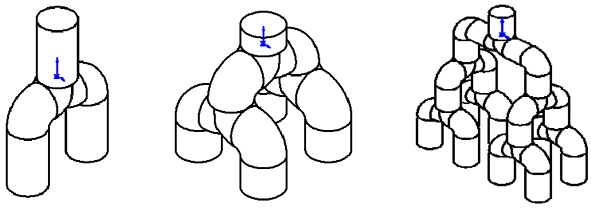

1-2 1-2-4 1-2-4-8

**Fig. 1: Examples of Circular Hole Dendritic Designs**

In order to investigate dendritic cooling systems it was necessary to characterise the pressure loss and internal heat transfer performance of the branching, curved internal passages, and the external heat transfer and film-cooling effectiveness experimentally over a range of engine representative conditions. Experiments were performed in a low speed wind tunnel where individual dendrites were supplied with pressurised air whilst the mainstream flow passed over the hole exits. It was possible to heat the coolant representative flow to drive heat transfer. The flow conditions were dimensionally matched over a range of real engine conditions. A transient liquid crystal technique allowed the assessment of the heat transfer coefficient distribution over the internal passages of the dendritic systems considered. The pressure loss characteristics of typical installed arrays of holes were measured during the experiments carried out above.

It is, of course near impossible to generate these cooling geometries using conventional manufacturing. The holes cannot be drilled or machined into the component after manufacture, and fabrication of a casting core for a conventional soluble core casting technique would be likely to result in low component yield. The method of manufacture envisaged for these components is that described in [13]. Here a rapid method for the production of casting cores using stereolithography of ceramic powder loaded resins is described. Although in its infancy, the method has already successfully produced components using high temperature alloys suitable for turbine blades and vanes. Beyond the scope this paper it has been shown that it is possible to manufacture novel cooling geometries of the type described in this paper with internally branching passages.

## NOMENCLATURE

| | |
|---|---|
| $A_{inlet}$ | Inlet hole Area to Dendritic system, m$^2$ |
| $BR$ | blowing ratio, $\dfrac{\rho U_c}{\rho U_m}$ |
| $C_D$ | discharge coefficient, $\dfrac{\dot{m}}{\sqrt{2\rho\Delta P}\left(A_{inlet}/n\right)}$ |
| $d$ | hole diameter, m |
| ***h*, *htc*** | heat transfer coefficient, W/ m$^2$ K |
| $K_L$ | Loss in dynamic head, $\dfrac{1}{C_d{}^2}-1$ |
| $k$ | thermal conductivity of air, W / m K |
| $m$ | slope of gas temperature signal K s$^{-1}$ |
| $\dot{m}$ | mass flow rate through single exit hole, kg / s |
| $MR$ | momentum ratio, $\dfrac{\rho U_c^2}{\rho U_m^2}$ |
| $n$ | number of exit holes in dendritic system |
| $Nu$ | **NUSSELT NUMBER,** $\dfrac{hd}{k}$ |
| $Nu_{db}$ | Nusselt number found using the Dittus Bolter relationship |
| $U_c$ | coolant exit velocity, m / s |
| $U_m$ | mainstream velocity ratio, m / s |
| $Re_{md}$ | Reynolds number based upon the cooling hole diameter, $\dfrac{\rho U_c d}{\mu}$ |
| $t$ | time, s |
| $T_{gas}$ | driving gas temperature, $^o$C |
| $T_{init}$ | initial model temperature, $^o$C |
| $T_{surface}$ | surface temperature, $^o$C |
| $x$ | thickness, m |
| $\alpha$ | thermal diffusivity |
| $\eta_f$ | film cooling effectiveness |
| $\rho$ | density, kg/m$^3$ |
| $\sqrt{\rho c k}$ | thermal product of substrate, W s$^{0.5}$ / m$^2$ K |
| $\mu$ | dynamic viscosity, Pa s |

## EXPERIMENTAL APPARATUS

The wind tunnel used in the experiments is a 500 x 500 mm square working section tunnel. The inlet flow, from atmosphere, passes through a number of screens and a honeycomb section before being accelerated through an area ratio of 4:1. A mesh heater is installed at the entrance to the working section which is able to supply 150 kW of heat to the mainstream flow. The walls of the working section are constructed from Perspex[1]. Tunnel speeds of up to 27 ms$^{-1}$ can be obtained. The freestream turbulence intensity is very low in the working section Tu < 0.1%. Previous measurements [14] have shown the flow velocity uniformity in the tunnel to be +/- 1% in the first metre of the working section.

In the current tests the average flow velocity was measured using a pitot-static probe. Data was acquired at 50 Hz from pressure transducers and thermocouples installed on the models and the tunnel. Pressure and temperature data were recorded using a 16 bit A/D convertor on a PC using a Labview driven program. This allowed flow conditions to be set accurately and transient changes in temperature to be recorded. Where digital video data was required this was simultaneously recorded at a frame rate of 25 Hz during the test. Synchronisation of the data

[1] Polymethylmethacrylate

was achieved by monitoring the voltage across an LED which appeared in the video images.

Models of the cooling system for the internal heat transfer studies were installed in the sidewall of the tunnel, which was fed with regulated dry air. The three dendritic cooling passage geometries shown in figure 1 were the subject of the current study. Importantly, as they have uniform hole diameter throughout, the dendritic systems tested were built up from single branching modules machined from Perspex (figure 2). In all cases the exits from the passages were aligned so that they formed spanwise rows of coolant holes exiting into the wind tunnel crossflow. A photograph of a 1-2-4-8 dendritic system with 3 flow branches between entrance and exit as installed in the tunnel side wall is shown as figure 3. The models were approximately 30 times engine scale. For each geometry the aim was to vary the inlet Reynolds numbers from 5000 to 15000, and blowing ratio from 0.5 to 1.

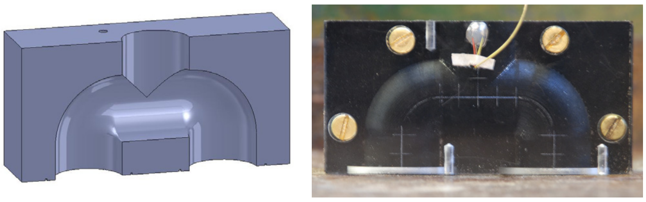

**Fig. 2: Modular Dendritic Blocks**

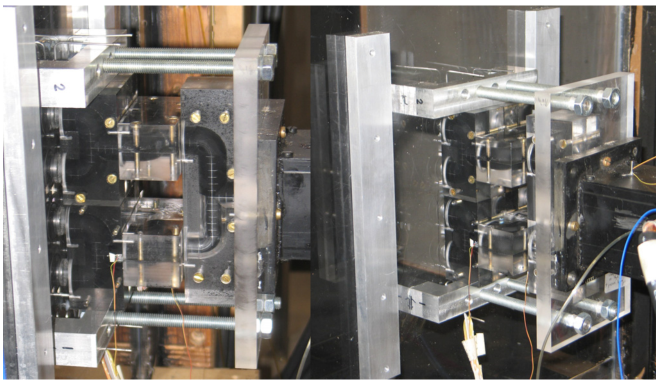

**Fig.3. Modular Dendritic Passage Arrangement**

The mass flow rate of air passing through the cooling geometry was fed from an independently regulated supply and measured using a BS1042 orifice meter, installed upstream of a second heater. This allowed independent heating of the coolant representative supply. All experiments were conducted at low speed in an incompressible flow regime, using air as the driving gas for both mainstream and coolant, as shown in figure 4.

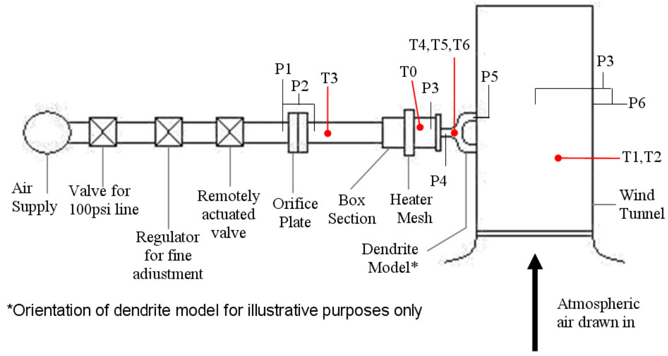


**Fig. 4: Experimental Setup with Thermocouple (prefix T) and Pressure Transducer Locations (prefix P)**

## LIQUID CRYSTAL TECHNIQUE

All local heat transfer coefficient distributions were measured using transient liquid crystal techniques. A thermally thin coating of thermochromic liquid crystals (TLCs) was used as a full surface thermometer applied to an insulating substrate. A technique using narrow band liquid crystals was selected because of the surface curvature. This method involved a processing technique where the 1-D heat conduction equation is solved for a semi-infinite solid, subject to a constant heat transfer coefficient convective boundary condition at the exposed surface, and an arbitrarily changing gas temperature which is at the initial solid temperature prior to the beginning of the test [15]. In the current tests it is the coolant representative flow that is heated in order to generate a significant and measurable temperature difference between the flow and the initial temperature of the dendritic model at the start of the test.

For the test surface to behave as a semi-infinite solid, the time taken for the full liquid crystal colour play to occur must be short compared to the time taken for the thermal pulse to travel through the wall of the test rig. Schultz and Jones [16] showed that the time, $t$, taken for the thermal pulse to travel across a wall of thickness, $x$, is calculated by

$$t = \frac{x^2}{16\alpha} \tag{1}$$

where $\alpha$ is the thermal diffusivity of the material and has a value of $1.08 \times 10^{-7}$ m$^2$/s for Perspex. With a Perspex plate of minimum thickness 0.010 m, heated from one side only, the maximum test time was thus calculated to be 58 s, where parallel branches are machined into a single piece of perspex, the separation distance is double this value and the limitation in test time remains 58 s. Typical tests were no longer than 30 s duration.

The solution is formed by modelling the gas temperature as the superposition of a series of offset ramps of slope $m$, such that if the gas temperature distribution is modelled as

$$T_{gas} = T_{initial} + \sum_{1}^{n} \Delta m_i (t - t_i) \bullet \mathrm{u}(t - t_i) \quad (2)$$

then [17] describe a solution for the surface temperature in the form:

$$T_{surface} = T_{initial} + \sum_{1}^{n} \Delta m_i (t - t_i) \left( 1 - \frac{2}{\frac{h\sqrt{t - t_i}}{\sqrt{\rho c k}} \sqrt{\pi}} + \frac{1 - e^{\frac{h^2 (t - t_i)}{\rho c k}} erfc\left( \frac{h\sqrt{t - t_i}}{\sqrt{\rho c k}} \right)}{\frac{h^2 (t - t_i)}{\rho c k}} \right) \quad (3)$$

The gas temperature used for the inlet and first branch of the dendritic system is measured using K-type gas 0.001" diameter wire thermocouples. Great care was taken to ensure the thermocouple bead was isolated from conduction losses to the wall of the plenum. The gas temperature at the entrance to subsequent branches of the dendritic system was determined by a heat flux versus wall temperature analysis of surface thermocouples mounted at the inlet to each branch.

The narrow band liquid crystals used in the dendritic passages undergo their full colour play over a range of 1 ºC, and are insensitive to both illumination and viewing angle. The liquid crystal colour play was calibrated prior to testing: nominally the two crystals used displayed peaks at 30 °C and 40 °C. Experimental intensity histories are produced using digital video cameras to capture the crystal colour play when the model is subjected to a sudden gas temperature change. In order to capture the full colour play throughout the 1-2-4 and 1-2-4-8 dendrites two video cameras were used, their viewing angles being 90$^o$ to one another. To ensure high quality results it was paramount to uniformly illuminate the test section; to do this a combination of fluorescent strip lights and angle poise lights were used, these had a uniform illumination temperature. The intensity histories produced were compared to analytical intensity histories generated for a range of heat transfer coefficients; the one with the minimum variance is selected as a solution. Figure 5 shows typical heat transfer coefficient distributions. Intensity history data are displayed at 3 points on the surface of the branch representing the full range of heat transfer coefficients measured in a single test. Excellent agreement is noted between the analytical and measured intensity data. This justifies the use of surface thermocouples to infer the driving gas temperature described above. The use of the full intensity signature ensured redundancy in the data used to create the fitted results. Using this technique an uncertainty of 7.7 - 7.9% is associated with the local *htc* and this is more fully reported in [15], this takes into account, uncertainty in the thermocouple offset and gain, both during the tests and calibration, the possible loss of video data during digitisation, the uncertainty in the thermal product of the perspex used in the test pieces, and the repeatability of the liquid crystal calibration.

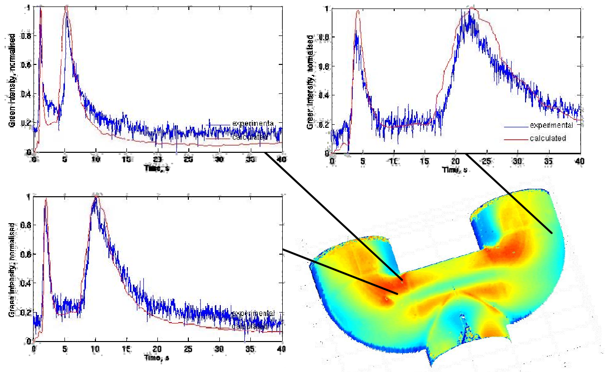


**Fig. 5: Experimental Time-Intensity Fits, Narrow Band Liquid Crystal technique**

## RESULTS

In total 36 separate branch sections were tested and analysed. For illustrative purposes only the local heat transfer coefficient distributions over the 1-2 inlet are presented in figure 6. Here it is appropriate to base the heat transfer coefficient on the local entry temperature to *each branch* of the dendritic system such that a general correlation can be formed based on the local Reynolds number in each dendrite

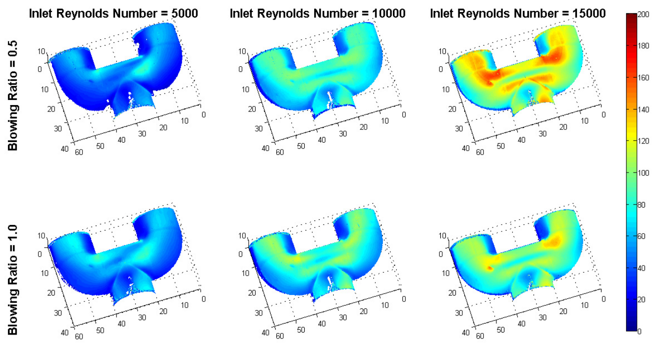


**Fig. 6: *htc* Distributions for a 1-2 Dendrite at a Range of Re numbers and BRs**

Over the entire dendrite's surface the *heat transfer coefficient* increases with increasing Reynolds number. Several stable repeatable features are visible in the local distributions. There is a characteristic pattern of impingement heat transfer on the branching surface beneath the inlet flow. Here the flow is extremely confined meaning that there is a strong shearing of the flow in the impingement region. At the highest Reynolds numbers this results in the maximum *htc* not at the stagnation point but in a distorted ring around it, associated, it is thought, with the turbulated flow spraying onto the thin boundary layer. The impingement wall jet wraps around the walls of the downstream branches and is subject to a cross branch pressure gradient. This vortical flow maintains a high *htc* as it is further accelerated towards the exit legs of each dendrite, see figure 7, figure 8 (a) and figure 9 (a). On the inlet branch of each dendrite there is an unexpected region of low heat transfer. It is speculated that this occurs because the flow separates from this surface: it does so because of blockage created by the initial recirculation of impinging flow.

The halving of the average velocity when the flow branches should lead to a drop in heat transfer, but this is only apparent on the outer shoulders of the dendrite and downstream of the corners where it is apparent that there is insufficient pressure gradient to fully turn the flow round the abrupt corner. The rest of this region benefits from the recirculation set up by the impinging flow.

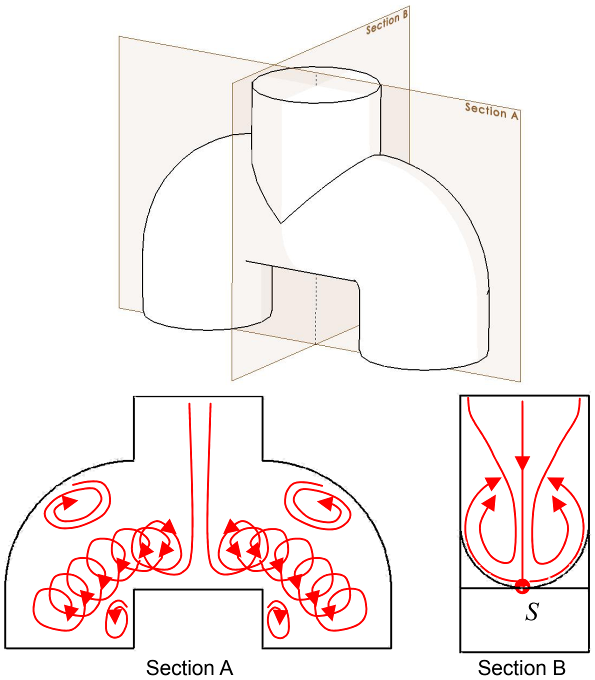


**Fig. 7: Cartoon of flow development from point of impingement**

Simple CFD of a 1-2 dendritic passage was used to provide diagnosis of the flow field and heat transfer features. A tetrahedral mesh (~600,000 elements) and size functions were used to model the coolant passages, flow was introduced through an inlet plenum and cross flow region at the exit of the branched pattern. The realisable *k-ε* model was used with standard wall functions. The results confirmed that at high Reynolds numbers the recirculating flow caused by the wall jet forms a highly shearing flow which scrubs against the side wall of the branch at mid-height before turning towards the exit (see figure 8 (a) and figure 9 (a)). The benefit is seen to be twofold with some of the recirculating flow from the impingement wall jet sweeping into the shoulder of the branches.

At low *Re* the typical impingement features are less pronounced. Here, there was little evidence of this recirculation and the flow from the centreline plane is strongly accelerated into the downstream legs, figure 8 (b). This forms a region of high heat transfer along the bottom surface of the branch (see figure 9 (b) and (c)). The turning of this flow forms a vortical structure that is confined to the middle of the passage and so generates little improvement in heat transfer in the downstream branches. The other notable difference compared to a high Reynolds number case is that the recirculation in the shoulder region appears much more stable.

While the CFD solution could not be relied on for accurate htc levels, the local distribution showed that the local *htc* was essentially symmetrical with respect to both geometric planes of symmetry, even in the presence of substantial cross flow (BR = 0.3). Thus it was justified to process only one view in experimental data.

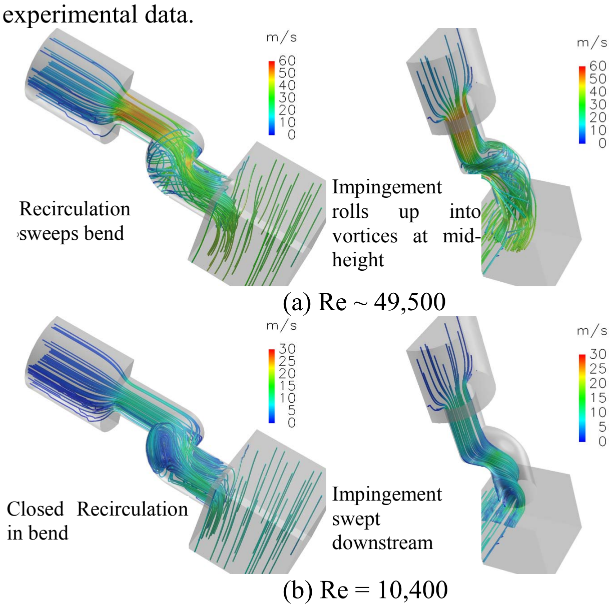


**Fig. 8: Pathlines at high and low Reynolds number 1-2 dendrite, BR=0.3, CFD Simulation**

The effect of the proximity of each dendritic branch to the inlet or outlet of the cooling system is primarily to drop the flow rate and slightly reduce the driving gas temperature. It is apparent that the heat transfer coefficient distributions follow a similar form from branch to branch. Figure 9 shows local Nusselt number distributions in a 1-2-4-8 dendritic system normalised by the average Nusselt number correlation presented below in equation 4. Here the inlet Reynolds number to the system is 15,000, and the local Reynolds number local to each branch is used to perform the normalisation. (It should be noted that the flow patterns and heat transfer distributions observed at the exit of one branch do not match the entrance to the subsequent branch in this viewing arrangement because the viewing angle of each is 90 degrees out of phase).

Of particular note in figure 9 is the lower, normalised Nusselt number in the entrance to the whole system when compared to the entrance of subsequent branches. It is inferred that the additional turbulence in the flow created as described above increases the Nusselt number in this region. The enhancement is of similar level in both the entrances to the 2$^{nd}$

and 3rd splits. The level of enhancement in the middle branch of the 1-2-4-8 split appears slightly higher than for the outermost branches. The reason for this is not yet understood.

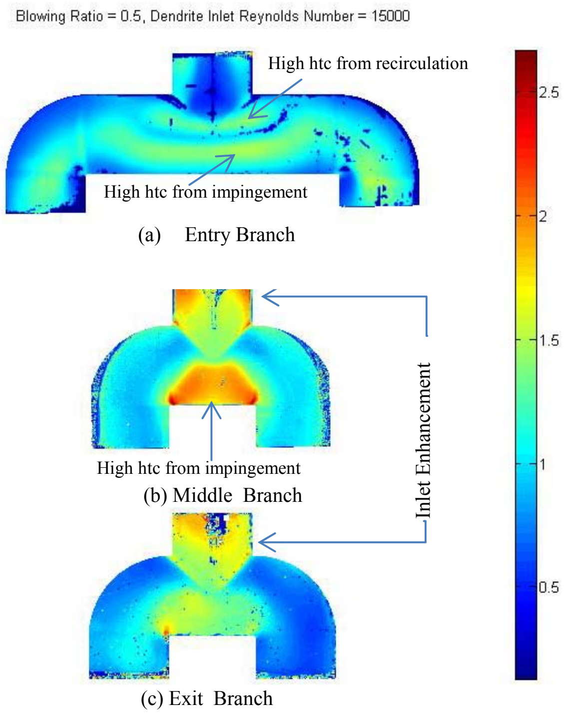


**Fig. 9: Normalised Nusselt number distribution for all branches in a 1-2-4-8dendrite**

Using the 36 heat transfer coefficient distributions and the inlet temperature of the coolant it was possible to calculate the average Nusselt number for each branch. The average Nusselt number is formed from an area weighted average of the local data. Because of passage curvature there is a variation in surface area of each pixel, and this is fully accounted for. Using local branch inlet *Re*, and normalising the Nusselt number by the Dittus-Boelter correlation for fully developed turbulent flow in smooth pipes the relationship below was found:

$$\frac{\overline{Nu}}{Nu_{db}} = 13.12\,Re^{-0.21} \tag{4}$$

The data and correlation are displayed in figure 10. The full performance of each system can then be determined by finding the average Nusselt number at the local Reynolds number of each branch in the dendritic system weighting the result total by the number of branches running at each local Reynolds number condition.

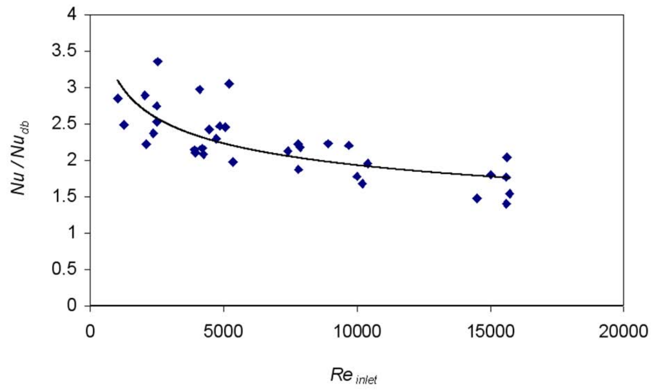


**Fig. 10: Local branch Reynolds number in a dendritic passage vs.** $Nu / Nu_{DB}$

Comparison to the work of other researchers is difficult as the wetted passage perimeter increases between the inlet and exit of the system.

A comparison is made between the summed product of local heat transfer coefficient and wetted surface area for each dendritic system and the values predicted by the correlation of Metzger and Codaro [18] for short film-cooling holes: this is shown in figure 11. Here the ratio of the summed *hA* product to two comparable straight hole cooling geometries is presented; these bound the range of possible cooling arrangements available using straight holes of identical diameter. The lower bound of achievable *hA* is represented by a single straight cooling hole spanning the same overall wall thickness. The upper bound is represented by a number of straight cooling holes, equal in number to the number of exits from each system: again the diameter remains constant. In both cases the mass flow rate is matched to the mass flow rate through the dendritic system. In considering figure 11 it is instructive to also consider the ratio of the wetted surface area between the dendritic systems and their comparators. This is included as table 1.

| Configuration | Wetted area ratio (dendrite / straight) | |
|---|---|---|
| | Matched Inlet | Matched Outlets |
| 1-2 | 1.95 | 0.98 |
| 1-2-4 | 2.93 | 0.73 |
| 1-2-4-8 | 4.90 | 0.61 |

**Table 1: Ratio of internal areas assuming the straight equivalents have either the same inlet or outlet cross sectional area**

It is notable that the highest *hA* enhancement seen cannot be attributed to the increased wetted surface area alone. The largest ratio of surface areas are created when comparing the 1-2-4-8 configurations. Also notable is that the enhancement factor is greater than 1 for very nearly all the results displayed. The authors would expect to replace a single cooling hole with a dendritic system is a real engine design, and so these figures of comparison are most instructive. For the highly branched systems (1-2-4) and (1-2-4-8) the comparison to a multiple hole system is necessarily unduly pessimistic. This is because the allowable packing density of such holes spanning the full thickness of the component would be sparser than for a dendritic design. Furthermore, to achieve the comparable mass flow rates used here the pressure ratio would have to be dramatically reduced for the multiple straight holes, and this is unfeasible when flow unsteadiness and possible flow ingestion are taken into account.

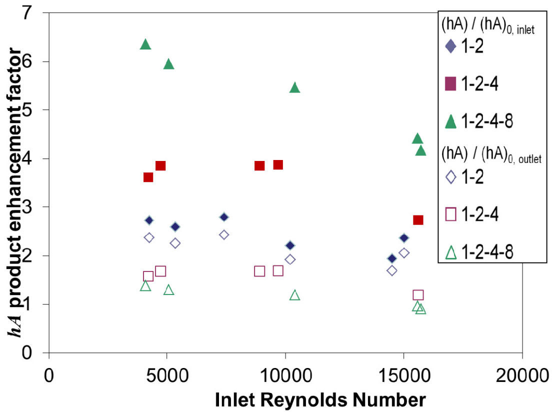


**Fig. 11: Average *hA* Product Enhancement Factor. Mass flow mass flow rate is matched for all ratios.**

## PRESSURE LOSS IN DENDRITIC PASSAGES

The pressure loss associated with different configurations of the large scale dendrites described above has been characterised. Measurements of pressure and mass flow rates were made over a range of engine representative blowing rates (BR = ∞ to 3) and inlet Reynolds numbers ($Re_{inlet}$ = 1000 – 15,000) which could be varied independently. For these tests the flow was unheated. The pressures were measured using Sensortechnics HCX010DH, HCX010DH, and HCX350DH, transducers and were digitised at 16 bit resolution. For each test, the velocity of the mainstream flow of the wind tunnel was held constant and the coolant mass flow rate was gradually increased such that the Reynolds number at the inlet to the dendritic passage increased from 0 to 15000 in small regular increments. After each increment the system was allowed to stabilise and a period of steady data extracted for analysis. Each reading was the average of approximately 100 data points.

Using the method of small perturbations of Moffatt [19] the root sum square uncertainty in the measured total pressure loss in inlet flow dynamic head was found be 2.05% over its full range, with the maximum worst case error being 4.11%.

## RESULTS

Figure 12 shows the variation in total pressure loss measured in inlet flow dynamic head for each of the dendritic configurations versus inlet Reynolds number at 3 different blowing ratios.

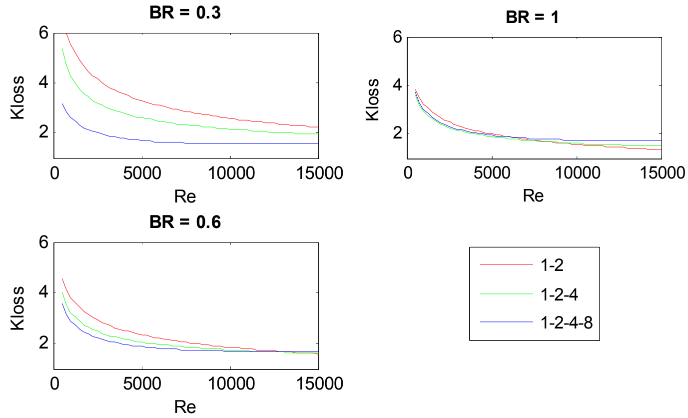


**Fig. 12 Variation in $K_L$ for a range of Re numbers at fixed BRs for the 3 dendritic configurations**

### Effect of Inlet Reynolds Number

The loss sensibly follows a well known inverse relationship found with inlet Reynolds number in the passage; a higher loss at the lowest Reynolds numbers is associated with laminar flow, while the levelling off of loss at a lower level is typical of fully turbulent flow. This behaviour is consistent over the range of BRs tested. Figure 13 confirms that the behaviour follows a sensible pattern, showing the change in discharge coefficient, $C_d$, with $Re_{inlet}$ for both a 1-2-4 dendrite with constant external crossflow and a straight cooling hole as tested by Hay [20], again with constant external crossflow. As would be expected the loss associated with a dendritic system is significantly greater than that of a conventional straight film cooling hole, and both sets of data follow the same form. It should be noted that the dendritic system has higher loss *by design*.

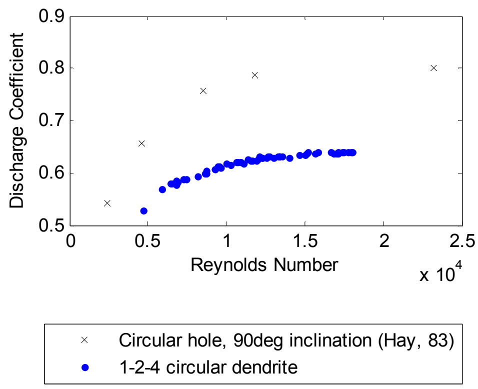


**Fig. 13. $C_d$ data comparison between current work and past studies**

### Effect of Exit Blowing Ratio

It is clear that as the blowing ratio is increased, the loss is reduced for a given dendritic configuration, and that this change is most pronounced for the single branch dendritic system. More surprisingly the dendritic systems with a higher number of branches have a lower loss at low blowing ratios.

The increases in the loss $K_{\text{loss}}$ can be attributed to the capping effect [21] of the mainstream flow on the exit of the film cooling holes. This is a mechanism whereby the mainstream flow effectively reduces the exit area of the hole and partially 'caps' the hole. The extent to which the exit area is reduced, or 'capped', is dependent upon the relative momentum ratios of the two flows involved.

If the momentum of the coolant is high relative to that of the mainstream (high *BR*); the coolant exiting cannot be instantaneously turned downstream by the mainstream flow. However at lower momentum ratios this capping mechanism has the effect of reducing the exit area of the coolant holes: with the flow area reduced and the velocity of the exit flow set by the driving pressure difference, the mass flow rate delivered is reduced. Thus the resultant discharge coefficient is also reduced.

While the proportional reduction in the exit area of the hole is independent of internal geometry at a given BR (based upon the exit velocity of the coolant), the ratio of the change in area to the throat area in each dendritic system is not. In the case of the 1-2 split, clearly the capping effect is dominant, and the throat must now lie at the exit of the system. However as each additional branch doubles the exit area, the proportion of the exit area that must be capped to cause a significant flow obstruction increases, and the loss for the 1-2-4-8 split at $BR = 1$ is approximately 50% of that for the 1-2 dendrite. Interestingly this also suggests that limited deposition of dust / sand / ash particulates in downstream dendritic branches is unlikely to substantially change the flow distribution through the dendrites.

Internally the loss associated with each branch is expected to scale with the local dynamic head, which drops by a factor of 4 with each additional branch. Thus the difference in internal loss between the 1-2, 1-2-4 and 1-2-4-8 dendritic systems would be expected to scale in the ratio 16 : 20 : 21 respectively. At most blowing ratios tested this difference appears to be small compared to the capping effect described above, however, at the highest Reynolds numbers and highest blowing ratios, the relative order of the loss is seen to follow this general pattern, suggesting that the holes are freely flowing into the crossflow.

## SUMMARY AND CONCLUSIONS

An experimental investigation has been carried out into the internal cooling performance of dendritic cooling systems. Two claimed benefits of dendritic cooling have been demonstrated: superior internal heat transfer coefficients and reduced exit blowing ratio for a given pressure margin through the cooling passage compared to conventional designs.

In the case of the improved internal heat transfer the average Nusselt number has been correlated to the branch inlet Reynolds number as $\overline{Nu}/Nu_{db} = 13.12Re^{-0.21}$. Furthermore it has been shown that in comparison to the expected Nusselt number of conventional straight cooling holes, typified by that estimated by Metzger and Cordaro [18], a dendritic system creates significantly higher *htcs*, in addition to the obvious increase in internal surface area.

The loss associated with flow passing through various dendritic configurations has been characterised. The loss performance has sensibly been shown to follow the trend with Reynolds number of other cooling hole configurations. More interestingly the variation in loss is a strong function of exit blowing ratio: particularly for dendritic systems with a small number of branches. Somewhat unexpectedly the loss does not increase sharply with increasing numbers of branches, and in fact the converse is generally true, with the singly branched dendrites having a higher loss at engine representative Reynolds numbers and blowing ratios.

An inference from the pressure loss and *hA* product data is that improved internal heat transfer performance can be achieved at the same overall pressure margin as used in conventional cooling designs, with a very significant drop in the velocity of the cooing film being ejected onto the external surface.


## ACKNOWLEDGMENTS

The EPRSC, Rolls-Royce and the UK government through the TSB funded this research: their contributions are gratefully acknowledged. Thanks also go to Gerald Walker and Trevor Godfrey of the Osney lab who manufactured and instrumented the test rig.


## REFERENCES


[1] Horlock, J.H., Watson, D. T., Jones, T.V., 2001. "Limitations on Gas Turbine Performance Imposed by Large Turbine Cooling Flows," *Journal of Engineering for Gas Turbines and Power*, **123**, pp 487-494.

[2] Eckert, E.R.G., Cho, H.H., 1994. "Transition from Transpiration to Film Cooling," *International Journal of Heat and Mass Transfer*, **37**, pp. 3 – 8.

[3] Battisti, L., Fedrizzi, R., Cerri, G., 2006. "Novel Technology for Gas Turbine Blade Effusion Cooling," Proceedings of GT2006, ASME Turbo Expo 2006, Power for Land, Sea and Air, GT2006-90516.

[4] Arcangeli, L., Surace, M., Tarcho, L., Coutandin, D., Zecchi, S., 2006. "Correlative analysis of effusion cooling systems," Proceedings of GT2006, ASME Turbo Expo 2006, Power for Land, Sea and Air, GT2006-90405.

[5] Gillespie, D.R.H., 1996. "Intricate Internal Cooling Systems for Gas Turbine Blading," D.Phil Thesis, University of Oxford

[6] Immarigeonk, A., Hassan, I., 2006. “An Advanced Impingement / Film Cooling Scheme for Gas Turbines – numerical study,” *International Journal of Numerical Methods for Heat & Fluid Flow*, **16**, pp. 470-493

[7] Sargison, J. E., Oldfield, M. L. G., Guo, S. M., Lock, G. D., Rawlinson, A. J., 2005. “A Converging Slot-Hole Film-Cooling Geometry—Part 1: Low-Speed Flat-Plate Heat Transfer and Loss,” *Journal of Turbomachinery*, **124**, pp. 453- 459

[8] Sargison, J. E., Oldfield, M. L. G., Guo, S. M., Lock, G. D., Rawlinson, A. J., 2005. “Flow visualisation of the external flow from a converging slot-hole film-cooling geometry,” *Experiments in Fluids,* **38**, pp 304-318.

[9] Liu, C.L., Zhu, H.R., Bai, J.T., Xu, D.C., 2009. “Experimental research on the thermal performance of converging slot holes with different divergence angles,” *Experimental Thermal and Fluid Science*, **33**, pp. 808–817.

[10] Liu, C.L., Zhu, H.R., Bai, J.T., Xu, D.C., 2010. “Film cooling performance of converging slot-hole rows on a gas turbine blade,” *International Journal of Heat and Mass Transfer*, **53**, pp. 5232–5241

[11] Nowlin, S.C., 2009. “The Use of Intersecting Film Cooling Passages for Nozzle Guide Vane Cooling,” D.Phil Thesis, University of Oxford

[12] Dieberger, J. A. (1978) Coolable Wall. United State Patent 4,118,146

[13] Frasier, D.J., Schlienger, M.E., Vessely, P.A., 2010. “Method and Apparatus for Production of a Cast Component,” US 7,779,890 B2, United States Patent

[14] Nowlin, S.R., Gillespie, D.R.H., Ireland, P.T., 2005. “A Transient Calorimeter Technique for Determining Regional Heat Transfer Coefficients in the Three-Temperature Flowfield at a Turbine Airfoil Leading Edge,” 50th ASME Turbo-Expo, **3**, pp. 729-738

[15] Abu Talib, A.R, Neely, A.J., Ireland, P.T., Mullender, A.J., 2004. “A Novel Liquid Crystal Image Processing Technique Using Multiple Gas Temperature Steps to Determine Heat Transfer Coefficient Distribution and Adiabatic Wall Temperature,” *Journal of Turbomachinery*, **126**, pp.587-595

[16] Schultz, D.L., Jones, T.V., 1973. “Heat transfer measurements in short-duration hypersonic facilities,” AGARD AG-165

[17] Ireland, P.T., Jones, T.V., 2000. “Liquid Crystal Measurements of Heat Transfer and Surface Shear Stress,” Measurement Science and Technology, **11**, pp969-966

[18] Metzger D.,E., Cordaro, J.V., 1979. “Heat Transfer in Short Tubes Supplied from a Cross-Flowing Stream,” ASME paper 79-WA/HT-16.

[19] Moffat, R.J., 1982. “Contributions to the theory of single sample uncertainty analysis,” *Journal of Fluids Engineering*, **104**, pp. 250.

[20] Hay, N., Lampard, D., Benmansour, S., 1983. “Effect of Cross-Flow on the Discharge Coefficient of Film Cooling Holes,” *Journal of. Engineering. for Power*, **105**, pp. 243–248

[21] Rowbury, D.A., Oldfield, M.L.G., Lock, G.D., 2001. “Large-Scale Testing to Validate the Influence of External Crossflow on the Discharge Coefficients of Film Cooling Holes,” *Journal of Turbomachinery*, **123**, pp.593-599